

UC Riverside

UC Riverside Previously Published Works

Title

Biodegradable Kojic Acid-Based Polymers: Controlled Delivery of Bioactives for Melanogenesis Inhibition

Permalink

<https://escholarship.org/uc/item/1fq2z6wn>

Journal

Biomacromolecules, 18(2)

ISSN

1525-7797

Authors

Faig, Jonathan J
Moretti, Alysha
Joseph, Laurie B
[et al.](#)

Publication Date

2017-02-13

DOI

10.1021/acs.biomac.6b01353

Peer reviewed



Published in final edited form as:

Biomacromolecules. 2017 February 13; 18(2): 363–373. doi:10.1021/acs.biomac.6b01353.

Biodegradable Kojic Acid-Based Polymers: Controlled Delivery of Bioactives for Melanogenesis Inhibition

Jonathan J. Faig[†], Alysha Moretti[†], Laurie B. Joseph[‡], Yingyue Zhang[†], Mary Joy Nova[§], Kervin Smith[§], and Kathryn E. Uhrich^{*†,ID}

[†]Department of Chemistry and Chemical Biology, Rutgers University, Piscataway, New Jersey 08854, United States

[‡]Ernest Mario School of Pharmacy, Rutgers University, Piscataway, New Jersey 08854, United States

[§]Department of Chemical & Biochemical Engineering, Rutgers University, Piscataway, New Jersey 08854, United States

Abstract

Kojic acid (KA) is a naturally occurring fungal metabolite that is utilized as a skin-lightener and antibrowning agent owing to its potent tyrosinase inhibition activity. While efficacious, KA's inclination to undergo pH-mediated, thermal-, and photodegradation reduces its efficacy, necessitating stabilizing vehicles. To minimize degradation, poly(carbonate-esters) and polyesters comprised of KA and natural diacids were prepared via solution polymerization methods. *In vitro* hydrolytic degradation analyses revealed KA release was drastically influenced by polymer backbone composition (e.g., poly(carbonate-ester) vs polyester), linker molecule (aliphatic vs heteroatom-containing), and release conditions (physiological vs skin). Tyrosinase inhibition assays demonstrated that aliphatic KA dienols, the major degradation product under skin conditions, were more potent than KA itself. All dienols were found to be less toxic than KA at all tested concentrations. Additionally, the most lipophilic dienols were statistically more effective than KA at inhibiting melanin biosynthesis in cells. These KA-based polymer systems deliver KA analogues with improved efficacy and cytocompatible profiles, making them ideal candidates for sustained topical treatments in both medical and personal care products.

Graphical abstract

*Corresponding Author. Address: Department of Chemistry and Chemical Biology, Rutgers, The State University of New Jersey, 610 Taylor Road Piscataway, NJ 08854-8087, USA. keuhrich@rutgers.edu; Tel.: (848) 445-0361; Fax: (732) 445-7036.

ORCID

Kathryn E. Uhrich: 0000-0001-7273-7528

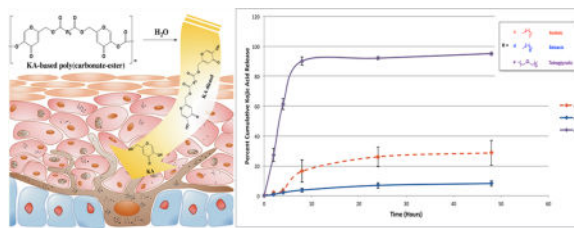
ASSOCIATED CONTENT

Supporting Information

The Supporting Information is available free of charge on the ACS Publications website at DOI: 10.1021/acs.biomac.6b01353.

KA-based polyester (6) degradation under skin conditions as well as polymer cytotoxicity analyses (5 and 6) (PDF)

The authors declare no competing financial interest.



INTRODUCTION

Tyrosinase is a copper-containing enzyme and key regulator of melanin biosynthesis, which catalyzes distinct reactions in the melanogenic cascade.¹ More specifically, tyrosinase facilitates the hydroxylation of L-tyrosine to L-dihydroxyphenylalanine (L-DOPA) and subsequent L-DOPA oxidation in concerted or concurrent steps initiating melanin biosynthesis.^{1–3} Thus, considerable research has focused on tyrosinase inhibition to reduce melanin overexpression.^{3,4} Melanin overexpression is associated with various skin hyperpigmentation disorders ranging from benign freckles and lentigo to melasma. While sun overexposure is frequently linked to hyperpigmentation disorders, the cause of melasma, which affects millions worldwide, is still not established.^{5,6} Moreover, upon onset of melasma, treatment is difficult to return skin to its normal pigment.⁷

Extensive research has been conducted on tyrosinase inhibitors as agents to overcome hyperpigmentation disorders.^{8–12} Kojic acid (KA), one such tyrosinase inhibitor, is a naturally occurring fungal metabolite derived from *Aspergillus*, *Penicillium*, and *Acetobacter* genera.¹³ KA's potency is well established in literature, resulting in its prominence as a positive control in both tyrosinase and melanin inhibition studies.¹² *In vitro* analyses has suggested its competitive inhibition activity stems from copper chelation in the active site of tyrosinase.¹⁴ Additionally, studies have shown KA to be a viable antioxidant and act as a radio-protective agent in both its natural form and metal complexes.^{15,16}

KA's efficacious properties have also resulted in researchers investigating polymeric and inorganic controlled delivery systems for KA in personal care and biomaterial applications.^{17,18} For example, KA-loaded magnetic nanoparticles demonstrated controlled release over 7 days, depending on the formulation.¹⁹ However, released KA showed significantly reduced antibacterial activity, suggesting KA degradation.¹⁹ In another example, KA was grafted onto chitosan oligosaccharides. Liu et al. demonstrated improved antibacterial activity in both Gram-positive and Gram-negative bacteria following KA's conjugation to chitosan as a pendant group.²⁰ KA-eluting ZnAl-hydrotalcite derivatives were found to release 68% KA over 8 h while improving photostability.²¹

While effective, KA's inclination to undergo pH-, photo-, and thermal-induced oxidation hampers its efficacy.²² Moreover, KA oxidation and metal chelation via its *alpha*-hydroxy ketone moiety in both solution and personal care formulations causes browning and decreases tyrosinase inhibition activity. Thus, researchers have investigated KA analogues and materials with enhance stability. Most notably, extensive studies have been conducted on

KA esters,^{23–26} specifically KA dipalmitate, which has been shown to increase stability in formulations.^{27,28}

Previous research has demonstrated that thermal and photolabile antioxidants can be stabilized via chemical incorporation into a polymer backbone.^{29–31} Building upon this knowledge, this work describes the synthesis and characterization of biodegradable, KA-based poly(carbonate-esters), and polyesters that hydrolytically degrade, releasing the tyrosinase inhibitor in a controlled manner. Hydrolytic degradation studies demonstrated that KA release was influenced by the chemical bond (i.e., carbonate vs ester) surrounding the enol functionality. Mushroom tyrosinase inhibition assays demonstrated that released KA maintains its bioactivity in addition to dienols possessing activity. Polymer and monomer cytotoxicity studies established appropriate concentrations for administration, all of which were therapeutically relevant. Additionally, melanin inhibition studies with B16 melanoma cells elucidated appropriate concentrations for topical use.

MATERIALS AND METHODS

Materials

1N hydrochloric acid (HCl), polytetrafluoroethylene (PTFE), and poly(vinylidene fluoride) (PVDF) syringe filters, and Wheaton glass scintillation vials were purchased from Fisher Scientific (Fair Lawn, NJ). KA and azelaic acid were acquired from Acros Organics (Morris Plains, NJ). 1-Ethyl-3-(3-(dimethylamino)propyl)-carbodiimide (EDCI) was purchased from AK Scientific (Union City, CA). *p*-Methoxybenzyl chloride (PMB-Cl) was obtained from TCI (Portland, OR). 3,6,9-Trioxaundecandioic acid, dried by azeotropic distillation with toluene, and all other reagents, solvents, and fine chemicals were purchased from Aldrich (Milwaukee, WI) and used as received.

¹H and ¹³C NMR and FT-IR Spectroscopies

Varian 400 or 500 MHz spectrometers were used to record proton (¹H) and carbon (¹³C) nuclear magnetic resonance (NMR) spectra using deuterated chloroform (CDCl₃) with tetramethylsilane as an internal reference or deuterated dimethyl sulfoxide (DMSO-*d*₆) as a solvent and internal reference. Fourier transform infrared (FT-IR) spectra were obtained using a Thermo Nicolet/Avatar 360 spectrometer, with samples (1–3 wt %) ground and pressed with potassium bromide (KBr) into a disc using an IR pellet die (International Crystal Laboratories, Garfield, NJ) or solvent casted via dichloromethane (DCM) to acquire a thin film on sodium chloride (NaCl) plates. Each spectra was an average of 32 scans.

Molecular Weight

Polymer precursors were analyzed via mass spectrometry (MS) to determine molecular weights. A Finnigan LCQ-DUO equipped with Xcalibur software and an adjustable atmospheric pressure ionization electrospray ion source (API-ESI Ion Source) was used at a pressure of 0.8×10^{-5} Torr and 150 °C API. Samples dissolved in methanol (<10 µg/mL) were injected via a glass syringe. Gel permeation chromatography (GPC) was used to determine polymers **5c–5e** and **6c–6e** weight-averaged molecular weight (M_w) and polydispersity indices (PDI) using a Waters liquid chromatography system consisting of a

Series 2414 refractive index (RI) detector, a 1515 isocratic high performance liquid chromatography (HPLC) pump, and a 717plus autosampler. Automation of the samples and processing of the data was performed using a Dell OptiPlex GX110 computer running Waters Breeze Version 3.20 software. Samples were prepared for autoinjection by dissolving in DCM (10 mg/mL) and filtering through 0.45 μm PTFE syringe filters. Samples were resolved on a Jordi divinylbenzene mixed-bed GPC column (7.8×300 mm, Alltech Associates, Deerfield, IL) at 25 $^{\circ}\text{C}$, with DCM as the mobile phase at a flow rate of 1.0 mL/min. Molecular weights were calibrated relative to narrow polystyrene standards (Polymer Source Inc., Dorval, Canada).

To determine the M_w and PDI of **6a** and **6b**, GPC was employed using a Waters liquid chromatography system consisting of a 515 HPLC pump and 2414 RI detector with Empower software. Polymer samples were prepared for autoinjection by dissolving in dimethylformamide (DMF) with 0.1% trifluoroacetic acid (TFA, 10 mg/mL) and filtering through 0.45 μm PTFE syringe filters. Samples were resolved by 103 and 105 \AA gel columns (Polymer Laboratories, Amherst, MA) in series at 25 $^{\circ}\text{C}$, with DMF, containing 0.1% TFA, as the mobile phase at a flow rate of 0.8 mL/min. Molecular weights were calibrated relative to narrow polystyrene standards.

Thermal Properties

Differential scanning calorimetry (DSC) measurements were carried out on TA Instrument Q200 to determine melting (T_m) and glass transition (T_g) temperatures. Samples (4–6 mg) were heated under a nitrogen atmosphere from -40 to 100 $^{\circ}\text{C}$ at a heating rate of 10 $^{\circ}\text{C}/\text{min}$ and cooled to -40 $^{\circ}\text{C}$ at a rate of 5 $^{\circ}\text{C}/\text{min}$ with a two-cycle minimum. TA Instruments Universal Analysis 2000 software, version 4.5A, was used to analyze the data.

PMB-KA (2) Synthesis (Scheme 1)—PMB-KA was synthesized using a modified literature procedure.³² KA (**1**, 1.00 equiv) was dissolved in 50 mL anhydrous DMF under nitrogen. Anhydrous sodium carbonate (Na_2CO_3 , 2.10 equiv) and PMB-Cl (1.05 equiv) were added to the reaction flask equipped with a reflux condenser and heated to 50 $^{\circ}\text{C}$. Thin layer chromatography (TLC, ethyl acetate eluent) was used to monitor the reaction progress. Following KA consumption, the reaction was cooled to room temperature and solvent removed *in vacuo*. The resulting beige powder was triturated in 200 mL deionized (DI) water for 30 min and subsequently filtered. The residue was dried under vacuum overnight to acquire pure **2**.

Yield: 7.64 g, 77% (off-white powder). ^1H NMR (400 MHz, $\text{DMSO}-d_6$): δ 8.13 (s, 1H, Ar-H), 7.32 (d, 2H, Ar-H), 6.93 (d, 2H, Ar-H), 6.29 (s, 1H, Ar-H), 5.65 (t, 1H, -OH), 4.84 (s, 2H, $-\text{CH}_2$), 4.27 (d, 2H, $-\text{CH}_2$), 3.74 (s, 3H, $-\text{CH}_3$). ^{13}C NMR ($\text{DMSO}-d_6$): δ 173.7 (C), 168.4 (C), 159.7 (C), 147.0 (C), 141.6 (C), 130.5 (2C), 128.5 (C), 114.3 (2C), 111.6 (C), 70.8 (C), 59.8 (C), 55.6 (C). IR (KBr, cm^{-1}): 3311 (OH, alcohol), 1652 and 1617 (C=C).

PMB-KA Diester (3) Synthesis (Scheme 1)—PMB-KA (**2**, 2.0 equiv), Diacid (1.0 equiv), and 4-dimethylaminopyridine (DMAP, 2.2 equiv) were dissolved in 20 mL anhydrous DCM to which EDCI (3.0 equiv) was added. TLC (ethyl acetate eluent) was used to monitor reaction progress. Following PMB-KA consumption, the reaction mixture was

diluted with DCM (80 mL) and washed with 10% potassium bisulfate (3 × 100 mL) and saturated sodium bicarbonate (3 × 100 mL). The organic layer was collected, dried over MgSO₄, isolated via vacuum filtration, and concentrated *in vacuo* to acquire pure **3**.

PMB-KA (Succinate) Diester (3a)—Succinic acid was used as the diacid. Yield: 1.20 g, 86% (white powder). ¹H NMR (400 MHz, DMSO-*d*₆): δ 8.19 (s, 2H, Ar-H), 7.32 (d, 4H, Ar-H), 6.93 (d, 4H, Ar-H), 6.43 (s, 2H, Ar-H), 4.95 (s, 4H, CH₂), 4.83 (s, 4H, CH₂), 3.74 (s, 6H, OCH₃), 2.69 (t, 4H, CH₂). ¹³C NMR (CDCl₃): δ 174.4 (2C), 172.0 (2C), 161.3 (2C), 159.8 (2C), 147.2 (2C), 141.8 (4C), 129.6 (2C), 127.7 (2C), 114.2 (4C), 114.1 (2C), 71.8 (2C), 61.0 (2C), 55.3 (2C), 33.6 (2C), 24.1 (2C). IR (NaCl, cm⁻¹): 1728 (C=O, ketone and ester), 1651 and 1618 (C=C). MS: *m/z* = 629.0 [M + 23].

PMB-KA (Adipate) Diester (3b)—Adipic acid was used as the diacid. Yield: 1.06 g, 87% (white powder). ¹H NMR (500 MHz, CDCl₃): δ 7.54 (s, 2H, Ar-H), 7.31 (d, 4H, Ar-H), 6.90 (d, 4H, Ar-H), 6.41 (s, 2H, Ar-H), 5.01 (s, 4H, CH₂), 4.88 (s, 4H, CH₂), 3.79 (s, 6H, OCH₃), 2.42 (t, 4H, CH₂), 1.70 (t, 4H, CH₂). ¹³C NMR (CDCl₃): δ 174.4 (2C), 171.0 (2C), 161.0 (2C), 159.8 (2C), 147.1 (2C), 141.7 (4C), 129.6 (2C), 127.6 (2C), 114.3 (4C), 114.1 (2C), 71.7 (2C), 61.4 (2C), 55.3 (2C), 28.5 (2C). IR (NaCl, cm⁻¹): 1725 (C=O, ketone and ester), 1651 and 1621 (C=C). MS: *m/z* = 656.9 [M + 23].

PMB-KA (Azelate) Diester (3c)—Azelaic acid was used as the diacid. Yield: 2.45 g, 95% (white powder). ¹H NMR (400 MHz, CDCl₃): δ 7.51 (s, 2H, Ar-H), 7.29 (d, 4H, Ar-H), 6.87 (d, 4H, Ar-H), 6.39 (s, 2H, Ar-H), 4.98 (s, 4H, CH₂), 4.85 (s, 4H, CH₂), 3.78 (s, 6H, OCH₃), 2.37 (t, 4H, CH₂), 1.62 (m, 4H, CH₂), 1.31 (m, 8H, CH₂). ¹³C NMR (CDCl₃): δ 174.4 (2C), 172.5 (2C), 161.5 (2C), 159.8 (2C), 147.1 (2C), 141.7 (4C), 129.6 (2C), 129.6 (2C), 114.1 (4C), 114.0 (2C), 71.7 (2C), 60.9 (2C), 55.3 (2C), 33.8 (2C), 28.8 (3C), 24.6 (2C). IR (NaCl, cm⁻¹): 1747 (C=O, ester and ketone), 1656 and 1613 (C=C), and 1515 (C-C, aromatic). MS: *m/z* = 699.2 [M + 23].

PMB-KA (Sebacate) Diester (3d)—Sebacic acid was used as the diacid. Yield: 3.26 g, 96% (white powder). ¹H NMR (400 MHz, CDCl₃): δ 7.51 (s, 2H, Ar-H), 7.30 (d, 4H, Ar-H), 6.87 (d, 4H, Ar-H), 6.40 (s, 2H, Ar-H), 4.99 (s, 4H, CH₂), 4.85 (s, 4H, CH₂), 3.79 (s, 6H, OCH₃), 2.37 (t, 4H, CH₂), 1.63 (m, 4H, CH₂), 1.30 (m, 8H, CH₂). ¹³C NMR (CDCl₃): δ 174.4 (2C), 172.6 (2C), 161.6 (2C), 159.8 (2C), 147.1 (2C), 141.7 (4C), 129.6 (2C), 129.6 (2C), 114.1 (4C), 114.0 (2C), 71.7 (2C), 60.9 (2C), 55.3 (2C), 33.8 (2C), 28.9 (4C), 24.7 (C). IR (NaCl, cm⁻¹): 1732 (C=O, ester and ketone), 1651 and 1621 (C=C), and 1519 (C-C, aromatic). MS: *m/z* = 713.4 [M + 23].

PMB-KA (Tetraglycolate) Diester (3e)—3,6,9-Trioxaundecandioic acid (tetraglycolic acid) was used as the diacid. The crude product was further purified by preabsorbing onto silica gel and performing flash chromatography using 100:0 → 60:40 ethyl acetate:acetone gradient. Yield: 1.71 g, 43% (white powder). ¹H NMR (400 MHz, CDCl₃): δ 7.50 (a, 2H, Ar-H), 7.25 (d, 4H, Ar-H), 6.82 (d, 4H, Ar-H), 6.37 (s, 2H, Ar-H), 4.92 (s, 4H, CH₂), 4.88 (s, 4H, CH₂), 4.19 (s, 6H, CH₃), 3.73 (s, 4H, CH₂), 3.67 (m, 4H, CH₂), 3.64 (m, 4H, CH₂). ¹³C NMR (CDCl₃): δ 174.3 (2C), 169.5 (2C), 160.8 (2C), 159.8 (2C), 147.8 (2C), 141.7 (4C), 129.6 (2C), 127.6 (2C), 114.4 (4C), 114.1 (2C), 71.7 (2C), 71.1 (2C), 70.6 (2C), 68.3

(2C), 61.2 (2C), 55.3 (C). IR (NaCl, cm^{-1}): 1765 (C=O, ester and ketone), 1651 and 1614 (C=C), and 1515 (C–C, aromatic). MS: $m/z = 733.1$ [M + 23].

KA Dienol (4) Synthesis (Scheme 1)—Compound **3** (1 equiv) was dissolved in anhydrous DCM (25 mL), and then anhydrous TFA (10 equiv) added.³² TLC (ethyl acetate eluent) was used to monitor reaction progress. Following **3** consumption, solvent was removed *in vacuo* and the resulting residue was triturated with ethyl acetate (20 mL), isolated via vacuum filtration, and dried *in vacuo* for 24 h.

KA (Succinate) Dienol (4a)—Yield: 1.05 g, 95% (white powder). ¹H NMR (400 MHz, DMSO-*d*₆): δ 9.23 (bs, 2H, –OH), 8.06 (s, 2H, Ar–H), 6.45 (s, 2H, Ar–H), 4.95 (s, 4H, CH₂), 2.69 (s, 4H, CH₂). ¹³C NMR (DMSO-*d*₆): δ 174.1 (2C) 171.8 (2C), 161.9 (2C), 146.5 (2C), 140.3 (2C), 112.9 (2C), 61.9 (2C), 28.8 (2C). IR (KBr, cm^{-1}): 3246 (OH, enol), 1744 (C=O, ester), 1728 (C=O, ketone), 1651 and 1628 (C=C). MS: $m/z = 365.3$ [M–1].

KA (Adipate) Dienol (4b)—Yield: 1.21 g, 95% (white powder). ¹H NMR (400 MHz, DMSO-*d*₆): δ 9.24 (bs, 2H, –OH), 8.09 (s, 2H, Ar–H), 6.47 (s, 2H, Ar–H), 4.96 (s, 4H, CH₂), 2.44 (t, 4H, CH₂), 1.58 (t, 4H, CH₂). ¹³C NMR (DMSO-*d*₆): δ 174.1 (2C) 172.6 (2C), 162.0 (2C), 146.5 (2C), 140.3 (2C), 112.9 (2C), 61.7 (2C), 33.2 (2C), 24.1 (2C). IR (KBr, cm^{-1}): 3246 (OH, enol), 1748 (C=O, ester), 1730 (C=O, ketone), 1653 and 1631 (C=C). MS: $m/z = 393.1$ [M–1].

KA (Azelate) Dienol (4c)—Yield: 1.08 g, 92% (off-white powder). ¹H NMR (400 MHz, DMSO-*d*₆): δ 9.20 (bs, 2H, –OH), 8.06 (s, 2H, Ar–H), 6.42 (s, 2H, Ar–H), 4.93 (s, 4H, CH₂), 2.37 (t, 4H, CH₂), 1.50 (m, 4H, CH₂), 1.24 (m, 6H, CH₂). ¹³C NMR (DMSO-*d*₆): δ 176.3 (2C), 174.9 (2C), 164.3 (2C), 148.7 (2C), 142.5 (2C), 115.1 (2C), 63.8 (2C), 35.7 (2C), 30.8 (3C), 26.7 (2C). IR (KBr, cm^{-1}): 3246 (OH, enol), 1746 (C=O, ester), 1732 (C=O, ketone), 1656 and 1633 (C=C). MS: $m/z = 435.4$ [M–1].

KA (Sebacate) Dienol (4d)—Yield: 1.89 g, 89% (off-white powder). ¹H NMR (500 MHz, DMSO-*d*₆): δ 9.21 (s, 2H, –OH), 8.06 (s, 2H, Ar–H), 6.42 (s, 2H, Ar–H), 4.93 (s, 4H, CH₂), 2.36 (t, 2H, CH₂), 1.51 (m, 2H, *J* = 16 Hz, R–CH=CH–R), 1.22 (s, 4H, CH₂), 3.84 (s, 6H, OCH₃). ¹³C NMR (DMSO-*d*₆): δ 176.2 (2C), 174.9 (2C), 164.3 (2C), 148.7 (2C), 142.5 (2C), 142.4 (2C), 115.1 (2C), 63.7 (2C), 35.7 (2C), 31.1 (2C), 30.9 (2C), 26.9 (2C). IR (KBr, cm^{-1}): 3265 (OH, enol), 1748 (C=O, ester), 1729 (C=O, ketone), 1646 and 1622 (C=C). MS: $m/z = 449.4$ [M–1].

KA (Tetraglycolate) Dienol (4e)—Yield: 0.513 g, 97% (white powder). ¹H NMR (500 MHz, DMSO-*d*₆): δ 9.22 (s, 2H, COOH), 8.07 (d, 2H, *J* = 16 Hz, R–CH=CH–R), 6.48 (s, 2H, Ar–H), 4.99 (d, 2H, *J* = 8 Hz, Ar–H), 4.23 (d, 2H, *J* = 8 Hz, Ar–H), 3.59 (d, 2H, *J* = 16 Hz, R–CH=CH–R), 3.53 (s, 4H, CH₂). ¹³C NMR (DMSO-*d*₆): δ 174.1 (2C), 170.1 (2C), 161.7 (2C), 146.5 (2C), 140.4 (2C), 113.1 (2C), 70.5 (2C), 70.1 (2C), 67.9 (2C), 61.8 (2C). IR (KBr, cm^{-1}): 3261 (OH, enol), 1745 (C=O, ester), 1739 (C=O, ketone), 1644 and 1620 (C=C). MS: $m/z = 469.0$ [M – 1].

KA Poly(carbonate-ester) (5) Synthesis—Polymer (5) was prepared using a modified solution polymerization (Scheme 2).³³ In brief, **4** (1.0 equiv) was dissolved in anhydrous DCM (20 mL) under argon and triethylamine (TEA, 4.4 equiv) added as a proton acceptor. The reaction mixture was cooled to 0 °C, after which triphosgene (1.0 equiv) dissolved in anhydrous DCM (5 mL) was added dropwise (10 mL/h). The reaction was allowed to stir at 0 °C until CO₂ evolution ceased (4 h). The reaction mixture was poured over chilled diethyl ether (400 mL) and the precipitate isolated via vacuum filtration. The residue was dissolved in anhydrous DCM, washed with acidic water (1 × 250 mL), dried over MgSO₄, concentrated to ~10 mL, and precipitated with an excess of chilled diethyl ether (400 mL). **5** was isolated via vacuum filtration and dried *in vacuo* at room temperature.

KA (Azelate) Poly(carbonate-ester) (5c)—Yield: 0.368 g, 60% (beige powder). ¹H NMR (400 MHz, CDCl₃): δ 8.17 (s, 2H, Ar-H), 6.52 (s, 2H, Ar-H), 4.95 (s, 4H, -CH₂), 2.41 (t, 4H, -CH₂), 1.66 (bm, 4H, -CH₂), 1.35 (b, 6H, -CH₂). ¹³C NMR (CDCl₃): δ 172.5 (2C), 171.5 (2C), 163.1 (2C), 148.9 (2C), 148.5 (2C), 141.4 (2C), 115.3 (2C), 60.9 (2C), 33.7 (2C), 28.7 (3C), 24.6 (2C). IR (NaCl, cm⁻¹): 1793 (C=O, carbonate), 1741 (C=O, ester and ketone), 1668 and 1636 (C=C). *M_w* = 18.8 kDa, PDI = 2.0. *T_g* = 26 °C.

KA (Sebacate) Poly(carbonate-ester) (5d)—Yield: 0.422 g, 54% (beige powder). ¹H NMR (400 MHz, CDCl₃): δ 8.14 (s, 2H, Ar-H), 6.52 (s, 2 H, Ar-H), 4.95 (s, 4H, CH₂), 2.41 (t, 4H, CH₂), 1.66 (m, 4H, CH₂), 1.32 (m, 8H, CH₂). ¹³C NMR (CDCl₃): δ 172.5 (2C), 171.5 (2C), 163.1 (2C), 148.9 (2C), 148.4 (2C), 141.4 (2C), 115.3 (2C), 60.7 (2C), 33.8 (2C), 28.9 (4C), 24.6 (2C). IR (NaCl, cm⁻¹): 1796 (C=O, carbonate), 1743 (C=O, ester and ketone), 1673 and 1643 (C=C). *M_w* = 18.0 kDa, PDI = 1.8. *T_g* = 15 °C.

KA (Tetraglycolic) Poly(carbonate-ester) (5e)—Yield: 0.466 g, 90% (light beige powder). ¹H NMR (500 MHz, CDCl₃): δ 8.16 (s, 2H, Ar-H), 6.54 (s, 2 H, Ar-H), 4.99 (s, 4H, CH₂), 4.26 (b, 4H, CH₂), 3.73 (b, 4H, CH₂), 3.67 (b, 4H, CH₂). ¹³C NMR (CDCl₃): δ 171.4 (2C), 169.5 (2C), 162.5 (2C), 148.7 (2C), 141.4 (2C), 139.3 (2C), 115.6 (2C), 71.1 (2C), 70.7 (2C), 68.3 (2C), 61.0 (2C). IR (NaCl, cm⁻¹): 1791 (C=O, carbonate), 1765 (C=O, ester), 1741 (C=O, ketone), 1673 and 1643 (C=C). *M_w* = 7.2 kDa, PDI = 1.1. *T_g* = 32 °C.

KA Polyester (6) Synthesis—Polymer (6) was prepared following Scheme 2. In brief, **4** (1.0 equiv) was dissolved 5 mL anhydrous DCM, unless noted otherwise, under argon and pyridine was (2.2 equiv) added. Adipoyl chloride (1.05 equiv), dissolved in 2 mL anhydrous DCM, was then added dropwise over 30 min. After stirring for 4 h the reaction was quenched with 25 mL 1 N HCl and poured into a separatory funnel. The organic layer was washed 2 × 50 mL 1 N HCl, 2 × 50 mL sat. NaHCO₃, dried over MgSO₄, and concentrated *in vacuo*. The polymer was dried under vacuum overnight to attain **6**.

KA (Succinate-co-adipate) Polyester (6a)—**4a** was dissolved in 5 mL anhydrous DMF at 50 °C. Crude polymer was purified by triturating in DCM and filtering to acquire **6a** as residue. Yield: 0.147 g, 54% (white powder). ¹H NMR (400 MHz, DMSO-*d*₆): δ 8.50 (s, 2H, Ar-H), 6.58 (s, 2H, Ar-H), 5.00 (s, 4H, CH₂), 2.72 (s, 4H, CH₂), 2.61 (bm, 4H, CH₂), 1.69 (bm, 4H, CH₂). ¹³C NMR (DMSO-*d*₆): δ 172.0 (2C), 171.8 (2C), 170.5 (2C), 163.3

(2C), 149.8 (2C), 140.9 (2C), 115.1 (2C), 61.6 (2C), 32.9 (2C), 28.7 (2C), 24.0 (2C). IR (KBr, cm^{-1}): 1765 and 1746 (C=O, ester), 1732 (C=O, ketone), 1667 and 1641 (C=C). M_w = 17.7 kDa, PDI = 1.2. T_g = 39 °C.

KA (Adipate) Polyester (6b)—4b was dissolved in 5 mL anhydrous DMF at 50 °C. Crude polymer was purified by triturating in DCM and filtering to acquire **6b** as residue. Yield: 0.121 g, 47% (white powder). ^1H NMR (400 MHz, $\text{DMSO}-d_6$): δ 8.50 (s, 2H, Ar-H), 6.57 (s, 2H, Ar-H), 4.99 (s, 4H, CH_2), 2.62 (bm, 4H, CH_2), 2.44 (bm, 4H, CH_2), 1.69 (bm, 4H, CH_2), 1.56 (bm, 4H, CH_2). ^{13}C NMR ($\text{DMSO}-d_6$): δ 172.6 (2C), 172.0 (2C), 170.5 (2C), 163.5 (2C), 149.8 (2C), 140.9 (2C), 115.1 (2C), 61.4 (2C), 33.1 (2C), 32.9 (2C), 24.1 (2C), 24.0 (2C). IR (KBr, cm^{-1}): 1756 and 1732 (C=O, ester), 1737 (C=O, ketone), 1666 and 1632 (C=C). M_w = 30.2 kDa, PDI = 1.3. T_g = 20 °C.

KA (Azelate-co-adipate) Polyester (6c)—Yield: 0.250 g, 96% (white powder). ^1H NMR (400 MHz, CDCl_3): δ 7.90 (s, 2H, Ar-H), 6.47 (s, 2H, Ar-H), 4.91 (s, 4H, CH_2), 2.65 (bm, 4H, CH_2), 2.39 (t, 4H, CH_2), 1.87 (bm, 4H, CH_2), 1.65 (bm, 4H, CH_2), 1.33 (bm, 6H, CH_2). ^{13}C NMR (CDCl_3): δ 172.4 (2C), 171.8 (2C), 170.1 (2C), 163.3 (2C), 150.4 (2C), 140.9 (2C), 115.1 (2C), 61.2 (2C), 33.1 (2C), 33.0 (3C), 24.3 (4C), 24.1 (2C). IR (NaCl, cm^{-1}): 1763 and 1754 (C=O, ester), 1739 (C=O, ketone), 1666 and 1639 (C=C). M_w = 9.2 kDa, PDI = 1.3. T_g = 4 °C.

KA (Sebacate-co-adipate) Polyester (6d)—Yield: 0.177 g, 71% (white powder). ^1H NMR (400 MHz, CDCl_3): δ 7.89 (s, 2H, Ar-H), 6.47 (s, 2H, Ar-H), 4.93 (s, 4H, CH_2), 2.65 (bm, 4H, CH_2), 2.40 (t, 4H, CH_2), 1.86 (bm, 4H, CH_2), 1.65 (bm, 4H, CH_2), 1.31 (bm, 8H, CH_2). ^{13}C NMR (CDCl_3): δ 172.0 (2C), 171.6 (2C), 170.4 (2C), 164.1 (2C), 149.7 (2C), 141.0 (2C), 115.0 (2C), 61.2 (2C), 33.2 (2C), 32.7 (4C), 24.2 (4C), 23.9 (2C). IR (NaCl, cm^{-1}): 1763 and 1752 (C=O, ester), 1737 (C=O, ketone), 1666 and 1638 (C=C). M_w = 9.0 kDa, PDI = 1.4. T_g = -1 °C.

KA (Tetraglycolate-co-adipate) Polyester (6e)—Yield: 0.200 g, 81% (white powder). ^1H NMR (400 MHz, CDCl_3): δ 7.91 (s, 2H, Ar-H), 6.50 (s, 2H, Ar-H), 5.00 (s, 4H, CH_2), 4.27 (s, 4H, CH_2), 3.76 (t, 4H, CH_2), 3.71 (t, 4H, CH_2), 2.65 (bm, 4H, CH_2), 1.85 (bm, 4H, CH_2). ^{13}C NMR (CDCl_3): δ 171.9 (2C), 170.8 (2C), 169.7 (2C), 163.1 (2C), 148.5 (2C), 141.1 (2C), 115.3 (2C), 71.7 (2C), 71.0 (2C), 68.5 (2C), 61.2 (2C), 32.9 (2C), 23.7 (2C). IR (NaCl, cm^{-1}): 1765 and 1754 (C=O, ester), 1737 (C=O, ketone), 1667 and 1639 (C=C). M_w = 9.6 kDa, PDI = 1.7. T_g = 10 °C.

Dienol (4) Log P Determination—Log P studies were conducted to investigate the relative hydrophobicity of dienols (**4**). Using HPLC equipped with an XTerra reverse-phase C_{18} (RP18) 3.5 μm 4.6 \times 150 mm column (Waters, Milford, MA) and Waters 2695 Separations Module, sample retention times were analyzed by a Waters 2487 Dual λ Absorbance Detector monitoring 254 and 270 nm. Mobile phases of HPLC grade methanol (MeOH) and 50 mM KH_2PO_4 with 1% formic acid in HPLC grade water were utilized at varying ratios (45:55 \rightarrow 60:40) and run at 1 mL/min flow rate and 25 °C.³⁴ All samples were first dissolved in DMSO and subsequently diluted in phosphate-buffer saline (PBS) to

1% DMSO and then filtered through 0.22 μm PVDF syringe filters prior to autoinjection (20 μL).

Dienol retention factor (k) for each mobile phase was calculated according to eq 1 (below), where t_R and t_0 are the retention times of the dienols and dead time, was determined by the injection of sodium nitrate, respectfully, and k_w was extrapolated (100% buffer).³⁴ Benzyl alcohol, 2-phenylethanol, methylparaben, anisole, and thymol were used as reference samples. Using these reference samples' of published $\log P_{o,w}$ values, a calibration curve was generated in which $\log P_{o,w}$ values were plotted on the y -axis with $\log k_w$ values, obtained from the same method as above, were plotted on the x -axis.^{35,36} Dienol $\log P$ values were then calculated from the curve using eq 2.

$$k_w = (t_R - t_0) / t_0 \quad (1)$$

$$\log P = \text{slope } x \log k_w + y - \text{intercept} \quad (2)$$

***In Vitro* KA Release**

KA release from polymer coatings ($n = 3$) was performed in phosphate-buffer saline (PBS, pH = 7.4, 37 °C), which represents physiological conditions, and a sodium acetate buffering system (pH = 5.5, 32 °C, skin surface conditions). Polymer coatings were prepared by dissolving polymer (50 mg) in anhydrous chloroform (5% w/v). The polymer solution (200 μL) was subsequently pipetted onto the bottom of 20 mL Wheaton glass scintillation vials (Fisher Scientific, Fair Lawn, NJ). The solvent was allowed to evaporate at ambient temperature and pressure overnight and placed under vacuum for an additional 24 h. Polymer coatings were incubated in 10 mL of either PBS or sodium acetate (buffers) with mild agitation (60 rpm) using a controlled environment incubator-shaker (New Brunswick Scientific Co., Edison, NJ). To maintain sink conditions, buffers (10 mL) were removed at predetermined time-points and replaced with fresh buffers. Buffer degradation products were analyzed and quantified via HPLC using an XTerra RP18 3.5 μm 4.6 \times 150 mm column (Waters, Milford, MA) by a Waters 2695 Separations Module equipped with a Waters 2487 Dual λ Absorbance Detector. Buffers were filtered through a 0.22 μm PVDF membrane prior to injection. A mobile phase of 15:85 acetonitrile and 50 mM KH_2PO_4 in HPLC grade water (Aldrich, Milwaukee, WI) with 1% formic acid at a flow rate of 1.0 mL/min was used to separate degradation media products at 25 °C. Polymer degradation product absorbance was monitored at 270 nm and KA release from the buffers was quantified based on calibration curves of KA, KA mono-enol, and KA dienol from known standard solutions. The percent cumulative KA release was calculated as the total KA release in the form of KA, KA mono-enol, and KA dienol.

Tyrosinase Inhibition In Mushroom Extracts

Small molecule dienols' (4a–e) tyrosinase inhibition activity were assayed using a modified protocol by Chen et al. and compared to that of free KA *in vitro*.⁹ Mushroom tyrosinase

inhibition was determined by adding dienols in sample media (25 μ L) to 96-well plates containing phosphate buffer (80 μ L, pH = 6.8) and 125 μ L substrate (0.5 mM L-DOPA) and incubated for 5 min at room temperature.⁹ Mushroom tyrosinase (20 μ L, 1250 U/mL, Sigma, Milwaukee, WI) in phosphate buffer (pH = 6.8) was added and incubated an additional 5 min at room temperature. The amount of dopachrome produced was measured using a microplate reader (Coulter, Boulevard Brea, CA) at 475 nm. Dienol (**4a–e**) tyrosinase inhibition was expressed as a function of the dienol concentration and inhibitory concentration 50 (IC₅₀) values calculated and compared to KA (positive control).

Cytotoxicity

In vitro studies were performed using 3T3 mouse fibroblasts in Dulbecco's Modified Eagle Medium (DMEM) supplemented with 10% fetal bovine serum, 1% penicillin/streptomycin, and 1% L-glutamate (culture medium) at 37 °C, 95% humidity, and 5% CO₂ (standard conditions). All polymers (**5a–5c**, **6a–6e**) and dienols (**4a–4e**) were solubilized in DMSO immediately prior to testing. The polymer-containing DMSO solutions were then diluted with culture medium to varying concentrations. Cells were seeded onto a 96-well tissue culture plate at 2000 cells/well in 100 μ L of medium for 24 h. Polymer-containing medium ranging from 0.1 mg/mL to 0.001 mg/mL concentration, dienol-containing medium ranging from 1 to 0.1 mM, or DMSO (control) were added to the cells and incubated under standard conditions. All experiments were conducted in triplicate ($n = 3$).

After 24 and 48 h, cell viability was determined using CellTiter 96 Aqueous One Solution Cell Proliferation Assay. Twenty microliters of 3-(4,5-dimethylthiazol-2-yl)-5-(3-carboxymethoxyphenyl)-2-(4-sulfophenyl)-2H-tetrazolium (MTS) reagent was added to each well and incubated for 4 h at 37 °C. The absorbance was determined using a microplate reader (Coulter, Boulevard Brea, CA) at 490 nm.

Melanin Inhibition

In vitro melanin inhibition studies were conducted using B16 melanoma cells (kindly provided by Dr. Jeffery Laskin, Rutgers University) in growth medium supplemented with 0.059% sodium bicarbonate and incubated under standard conditions.³⁷ To maintain logarithmic growth, cells were passaged every 3 days.

B16 melanoma cells were seeded onto a 12-well plate at 100 000 cells/well in 2 mL growth medium. After 48 h, the medium was removed and replaced with sample solutions (KA in DMSO, dienols in DMSO, or DMSO control) in growth medium at 1, 0.5, 0.1 mM. After 48 h, the treatment media was removed and cells trypsinized followed by centrifugation at 1100 rpm for 7 min at room temperature. Cell pellets were washed with PBS, then centrifuged at 1100 rpm for 7 min, and pellets were resuspended in 1 N NaOH with 10% DMSO. The cell pellets were heated to 80 °C for 1 h and cooled to room temperature. The absorbances of the resulting solutions were then measured using a microplate reader (Coulter, Boulevard Brea, CA) at 405 nm. All studies were conducted in triplicate and compared to positive (KA) control. DMSO was used as the negative control.

RESULTS AND DISCUSSION

Synthesis and Characterization

Poly(carbonate-esters) and polyesters, comprised of KA and linear diacids, were synthesized. Following previously published methods, PMB-KA (**2**) was prepared via a selective S_N2 reaction with PMB-Cl at the enolic site of KA.³² PMB-KA diesters (**3**) were subsequently synthesized via carbodiimide coupling using EDCI and DMAP. The diacids (succinic, adipic, azelaic, sebacic, of 3,6,9-trioxaundecanedioic acid) were reacted with PMB-KA to acquire **3**. The low purity of commercially available 3,6,9-trioxaundecanedioic acid (~70%) necessitated column chromatography to further purify the crude **3e**. KA dienols (**4**) were obtained following a modified procedure described by Chen et al., in which the PMB-moiety was selectively deprotected using TFA.³² Successful synthesis of **2** was confirmed by the absence of the enolic proton and appearance of PMB aromatic (7.32 and 6.93 ppm), benzyl (4.84 ppm), and methoxy protons (3.74 ppm, Figure 1A) and the aromatic functionality in both ^{13}C NMR and FTIR spectra. Using **3d** as an example, the structure was confirmed by the presence of linker methylene protons (2.37, 1.62, and 1.31 ppm, Figure 1B) in ^1H NMR spectrum and the ester functionality in both ^{13}C NMR and FTIR spectra. Subsequent deprotection to acquire **4d** was validated by the absence of the PMB peaks (Figure 1C) in ^1H NMR. MS corroborated the mass of polymer precursors (**3** and **4**).

Following isolation and characterization of **4**, KA poly(carbonate-esters) were synthesized by a modified solution polymerization with TEA as a proton acceptor and triphosgene as a coupling reagent.³³ In initial attempts, pyridine was used in place of TEA owing to its use in triphosgene-mediated solution polymerizations to acquire polycarbonates, however, it yielded low M_w oligomers in poor yield.³⁸ Furthermore, polymerization attempts with **4a** and **4b** resulted in insoluble systems and were not further characterized. Using **5d** as an example, dienol polymerization was confirmed by the downfield shift in olefin peaks of KA (Figure 1D) and by the appearance of the carbonate bond in ^{13}C NMR and FTIR spectra.

To chemically incorporate **4a** and **4b** into polymer systems, KA-based polyesters were explored. KA polyesters were synthesized following a modified procedure in which pyridine facilitated *O*-acylation of adipoyl chloride to acquire **6**.³⁹ Adipates were used due to the final degradation product, adipic acid, being generally regarded as safe by the FDA and has been used extensively in bioactive-based polymer systems.^{29,40} Using **6d** as an example, successful polymerization was indicated by the absence of the enolic proton and the appearance of new methylene peaks at 2.65 and 1.86 ppm (Figure 1E).

KA poly(carbonate-esters) molecular weights ranged from 7.2 to 18.8 kDa with aliphatic linked KA dienols producing higher M_w polymers (**5c–d**). Additionally, the linker composition and length was found to influence T_g , with heteroatom-containing polymer (**5e**) possessing the highest T_g and decreasing aliphatic linker length producing a higher T_g . The former trend may be due to the shorter C–O bond relative to C–C bond, which reduces the polymer flexibility, whereas the latter is consistent with the literature.^{40,41} KA polyesters had a lower M_w , with the exception of **6e**, when compared to KA poly(carbonate-ester) counterparts, with M_w ranging from 9.0–30.2 kDa. As expected, when comparing KA polyester and KA poly(carbonate-ester) T_g values derived from the same monomer, in

comparison the polyester had consistently lower T_g values. Again, this result is likely due to the enhanced flexibility from the additional adipate moiety in the polyester.

Dienol (4) log P Determination

Dienol (4) log P studies were conducted to both gain insight into water solubility and skin penetration. The dienol log P values were extrapolated from an HPLC method to determine lipophilicity.³⁵ Retention factors (k) were calculated according to eq 1 for each concentration of MeOH and the k_w values extrapolated based on the retention times (Table 1).

The calculated log P values in Table 1 followed the trend **4e** < **4a** < **4b** < **4c** < **4d**. As expected, **4e** was the most hydrophilic dienol, presumably due to the increase in oxygen content.³⁶ The remaining dienols followed a trend of increasing aliphatic content between the KA moieties, where longer aliphatic chains corresponded to a higher log P . All compounds possessed a log P value greater than KA, which has been reported as low as -1.11 and as high as -0.66.^{42,43}

In Vitro KA Release

KA poly(carbonate-ester) and polyester hydrolytic degradation was studied using polymer coatings to monitor KA release. Polymer coatings were immersed in PBS under physiological conditions (pH = 7.4, 37 °C) or sodium acetate buffer (pH = 5.5, 32 °C) to mimic skin conditions and polymer degradation separated using HPLC. KA (1), KA monoenoil (7), and KA dienol (4) concentrations were quantified at each time-point (Figure 2A).

KA poly(carbonate-esters) hydrolytically degraded through the carbonate bond, generating dienol (4), which subsequently underwent further hydrolysis to release KA (1) and the respective KA monoenoil (7), which was confirmed by HPLC (Figure 2A). Previous hydrolytic degradation studies using poly(carbonate-esters) suggested that the backbone composition influenced the susceptibility of ester vs carbonate toward hydrolysis.^{44,45} We hypothesized that the enhanced stability of the enol leaving group and hydrophilicity of the surrounding KA moieties promoted faster hydrolytic degradation of the carbonate functionality. Furthermore, upon initial hydrolysis at the carbonate site, an unstable carbonic acid forms; the literature has shown this compound to readily decarboxylate, releasing CO₂ and the alcohol-derivative.^{46,47} Using **5e** as an example, HPLC chromatograms displayed a peak at 2.18 min, corresponding to KA, with additional peaks at later retention times, representing monoenoil (7, 3.44 min) and dienol (4, 6.95 min, Figure 2B)

Under physiological conditions, the release profiles of KA poly(carbonate-esters) and polyesters were drastically influenced by the linker molecule and polymer composition. The water-miscible, hydrophilic 3,6,9-trioxaundecandioic acid linker of **5e** promoted >95% KA release within 8 h, whereas aliphatic linked **5c** and **5d** release rate was considerably slower at 29% and 8.3%, respectively, over the two day study (Figure 3). These trends are consistent with the dienol log P data; dienols with a lower log P degraded at faster rates (**5e** > **5c** > **5d**).

Whereas the KA-based poly(carbonate-esters) released three distinct degradation products (KA, enol, and dienol), KA-based polyesters released additional oligomeric degradation products. Thus, the polyester degradation media was allowed to further hydrolyze (~2 days) until quantifiable degradation products (e.g., KA, enol, and dienol) were present in the HPLC chromatograms. KA-based polyester degradation followed a similar trend as KA-based poly(carbonate-esters), that is, the more hydrophilic **6e** degraded the quickest with aliphatic linked **6a–6d** degrading slower with increasing aliphatic chain length (Figure 4). With the exception of **6d**, KA-based polyesters hydrolyzed statistically slower than their poly(carbonate-ester) counterparts. The increased aliphatic content of the polyester is hypothesized to increase their relative hydrophobicity, thus, reducing the release rates.

Media pH and temperature also had profound impacts on polymer degradation, with lower pH and lower temperature facilitating slower KA release from both poly(carbonate-esters) (Figure 5) and polyesters (Figure S1). These results are consistent with similar bioactive-based polymers in literature.^{31,48} Akin to the release study under physiological conditions, **5e** degraded most rapidly, releasing >70% bioactive in the first 8 h. Moreover, both KA-based poly(carbonate-esters) and polyesters possessed identical trends when compared to physiological conditions, with **4e**-based polymers degrading the quickest and the remaining polymers' release profiles following increasing aliphatic chain length.

Interestingly, the predominant degradation product for each of the KA-based poly(carbonate-esters) was dienol (Figure 6) under skin mimicking conditions. This result was consistent with the hypothesis that **5** degrades first at the carbonate bond, and subsequently at the ester moiety, to release KA. The enhanced stability of the ester moiety toward hydrolysis results in an accumulation of **4** under more acidic conditions. While the intended degradation product was KA, KA dienols (**4**) were shown to possess superior cytocompatibility and tyrosinase inhibition profiles (discussed below) compared to KA.

Similar to the studies conducted under physiological conditions, KA-based polyesters' (**6**) degradation media had additional oligomeric products that were allowed to further degrade (2 days) into quantifiable products. Collectively, the polyesters degraded statistically slower than poly(carbonate-esters) when comparing polymers derived from the same dienol (**4**) under skin mimicking conditions. Additionally, the poly(carbonate-esters) were able to generate sufficient concentrations of dienols to elicit a therapeutic response as indicated by the tyrosinase inhibition studies (shown below).

Mushroom Tyrosinase Inhibition

KA dienols (**4a–4e**) were the major degradation products observed under skin condition degradation, their tyrosinase inhibition IC₅₀ values were determined using a modified procedure with L-DOPA as a substrate.⁹ All dienols (**4a–4e**) possessed IC₅₀ values at μM levels (Table 2). Additionally, aliphatic linked dienols (**4a–4d**) had IC₅₀ values statistically lower than KA itself. This finding is promising since poly(carbonate-ester) degradation under skin conditions yields dienols as the major degradation product. Whereas aliphatic-linked dienols improved tyrosinase inhibition, the oxygen-containing linker of **4e** decreased its activity relative to KA.

Although **4e** was the least effective tyrosinase inhibitor of the compounds tested, the rapid degradation of its poly(carbonate-ester) derivative (**5e**) generated concentrations well above its IC₅₀ value (Figure 7). For example, during the *in vitro* release analysis of **5e** under skin conditions, dienol (**4e**) concentrations of 100 μM, 3-fold greater than **4e**'s IC₅₀, were generated by the initial 2 h time-point (Figure 7). By the 8 h time-point in the same study, **4e** concentration were 25-fold greater than the determined IC₅₀ (30 μM) value were (Figure 7). Moreover, while the degradation of **5c** is considerably slower than that of **5e**, it still generated dienol (**4c**) concentrations greater than its IC₅₀ value under *in vitro* skin conditions owing to the heightened tyrosinase inhibition activity of **4c** (Table 2).

Cytotoxicity

The dienols (**4a–4e**) displayed potent tyrosinase inhibition, IC₅₀ values, and were the major degradation product under skin conditions, their toxicity was investigated using 3T3 fibroblasts rather than B16 cells, as they more closely mimic normal cellular behavior. All dienols were found to be nontoxic up to 1 mM (Figure S2), which was well above their tyrosinase inhibition IC₅₀ values. Interestingly, KA was slightly cytotoxic after 48 h (Figure S3). More importantly, both **4c** and **4d** were cytocompatible at concentrations shown to inhibit melanin production (Figure 8).

To determine *in vivo* use parameters cytotoxicity studies were conducted on all polymers (**5** and **6**). 3T3 cells were incubated in the presence of polymers at 0.1, 0.01, and 0.001 mg/mL. DMSO was used as the control. Studies were performed over 48 h with cell viability monitored every 24 h.

Collectively, all KA poly(carbonate-esters) and polyesters were cytocompatible at 0.01 and 0.001 mg/mL over 48 h (Figure S4–S7). At 0.1 mg/mL, **5e** was found to be cytocompatible, whereas **5c** and **5d** were cytotoxic at 24 and 48 h (Figure S4 and S5, respectively), as well as all the KA-based polyesters were cytotoxic (**6a–6e**, Figure S6 and S7, respectively). These data suggest that the increased hydrophilicity of **5e**, as demonstrated by log *P* analysis, was responsible for the improved cytocompatibility while hydrophobic polymers were observed to cytotoxic in analogous systems.

Melanin Inhibition

Melanin inhibition studies were conducted on all dienols due to the enhanced tyrosinase inhibition activity of **4a–4d** (Table 2). It was observed that, **4e** was not superior at inhibiting melanin production, presumably due to its lower tyrosinase inhibition activity as compared to KA (Figure 8). Among the aliphatic-linked dienols, **4c** and **4d** were the most potent inhibitors of melanin production. We hypothesize that the increased activity of **4c** and **4d** could be due to their highly lipophilic nature, possibly facilitating passive cellular uptake. Additionally, both **4c** and **4d** were statistically superior to KA, which displayed no inhibition at the highest concentration tested (1 mM).

CONCLUSION

KA was successfully incorporated into diverse polymer backbones using solution polymerization to acquire poly(carbonate-esters) and polyesters containing varying linker molecules. KA-based polymers released bioactives in a controlled, sustained manner under physiological and skin conditions overtime. Interestingly, KA was the predominant degradation product under physiological conditions, whereas KA dienols (**4**) were the major degradation products under skin conditions. Further analysis demonstrated improved tyrosinase inhibition activity (lower IC₅₀) for aliphatic-linked dienols when compared to KA, while enhanced cytocompatibility was observed for all dienols. Moreover, cellular melanin inhibition studies identified lead dienols (**4c** and **4d**), which were found to be statistically superior to KA at inhibiting melanin production. These polymer systems are promising delivery vehicles, degrading into KA analogues with improved efficacy and cytocompatible profiles. Future studies will investigate enhancing the release rate of polymers into lead dienols to topically relevant timeframes, in addition to formulation and stability studies.

Supplementary Material

Refer to Web version on PubMed Central for supplementary material.

Acknowledgments

This work was supported by the U.S. Department of Education Graduate Assistance in Areas of National Need (GAANN) Fellowship (AM).

References

1. Slominski A, Tobin DJ, Shibahara S, Wortsman J. Melanin Pigmentation in Mammalian Skin and Its Hormonal Regulation. *Physiol. Rev.* 2004; 84:1155–1228. [PubMed: 15383650]
2. Solomon EI, Sundaram UM, Machonkin TE. Multicopper Oxidases and Oxygenases. *Chem. Rev.* 1996; 96:2563–2605. [PubMed: 11848837]
3. Kim YJ, Uyama H. Tyrosinase inhibitors from natural and synthetic sources: structure, inhibition mechanism and perspective for the future. *Cell. Mol. Life Sci.* 2005; 62(15):1707–23. [PubMed: 15968468]
4. Chang TS. An updated review of tyrosinase inhibitors. *Int. J. Mol. Sci.* 2009; 10(6):2440–75. [PubMed: 19582213]
5. Prignano F, Ortonne JP, Buggiani G, Lotti T. Therapeutical approaches in melasma. *Dermatol. Clin.* 2007; 25(3):337–42. viii. [PubMed: 17662899]
6. Sheth VM, Pandya AG. Melasma: a comprehensive update: part I. *J. Am. Acad. Dermatol.* 2011; 65(4):689–97. quiz 698. [PubMed: 21920241]
7. Gupta AK, Gover MD, Nouri K, Taylor S. The treatment of melasma: a review of clinical trials. *J. Am. Acad. Dermatol.* 2006; 55(6):1048–65. [PubMed: 17097400]
8. Kim Y, Chung JE, Kurisawa M, Uyama H, Kobayashi S. New Tyrosinase Inhibitors, (+)-Catechin-Aldehyde Polycondensates. *Biomacromolecules.* 2004; 5(2):474–479. [PubMed: 15003008]
9. Chen WC, Tseng TS, Hsiao NW, Lin YL, Wen ZH, Tsai CC, Lee YC, Lin HH, Tsai KC. Discovery of highly potent tyrosinase inhibitor, T1, with significant anti-melanogenesis ability by zebrafish in vivo assay and computational molecular modeling. *Sci. Rep.* 2015; 5:7995. [PubMed: 25613357]
10. Khatib S, Nerya O, Musa R, Shmuel M, Tamir S, Vaya J. Chalcones as potent tyrosinase inhibitors: the importance of a 2,4-substituted resorcinol moiety. *Bioorg. Med. Chem.* 2005; 13(2):433–41. [PubMed: 15598564]

11. Solano F, Briganti S, Picardo M, Ghanem G. Hypopigmenting agents: an updated review on biological, chemical and clinical aspects. *Pigm. Cell Res.* 2006; 19(6):550–71.
12. Lee SY, Baek N, Nam T. Natural, semisynthetic and synthetic tyrosinase inhibitors. *J. Enzyme Inhib. Med. Chem.* 2016; 31(1):1–13.
13. Leyden JJ, Shergill B, Micali G, Downie J, Wallo W. Natural options for the management of hyperpigmentation. *Journal of the European Academy of Dermatology and Venereology: JEADV.* 2011; 25(10):1140–5. [PubMed: 21623927]
14. Cabanes J, Chazarra S, Garcia-Carmona F. Kojic acid, a cosmetic skin whitening agent is a slow-binding inhibitor of catecholase activity in tyrosinase. *J. Pharm. Pharmacol.* 1994; 46(12):982–985. [PubMed: 7714722]
15. Emami S, Hosseinimehr SJ, Taghdisi SM, Akhlaghpour S. Kojic acid and its manganese and zinc complexes as potential radioprotective agents. *Bioorg. Med. Chem. Lett.* 2007; 17(1):45–8. [PubMed: 17049858]
16. Mitani H, Koshiishi I, Sumita T, Imanari T. Prevention of the photodamage in the hairless mouse dorsal skin by kojic acid as an iron chelator. *Eur. J. Pharmacol.* 2001; 411:169–174. [PubMed: 11137872]
17. Synytsya A, Blafková P, Synytsya A, opíková J, Sp vá ek J, Uher M. Conjugation of kojic acid with chitosan. *Carbohydr. Polym.* 2008; 72(1):21–31.
18. Liu X, Xia W, Jiang Q, Xu Y, Yu P. Effect of kojic acid-grafted-chitosan oligosaccharides as a novel antibacterial agent on cell membrane of gram-positive and gram-negative bacteria. *J. Biosci. Bioeng.* 2015; 120(3):335–9. [PubMed: 25682520]
19. Hussein-Al-Ali SH, El Zowalaty ME, Hussein MZ, Ismail M, Dorniani D, Webster TJ. Novel kojic acid-polymer-based magnetic nanocomposites for medical applications. *Int. J. Nanomed.* 2014; 9:351–62.
20. Liu X, Xia W, Jiang Q, Xu Y, Yu P. Synthesis, characterization, and antimicrobial activity of kojic acid grafted chitosan oligosaccharide. *J. Agric. Food Chem.* 2014; 62(1):297–303. [PubMed: 24364425]
21. Ambrogi V, Peroli L, Nocchetti M, Latterini L, Pagano C, Massetti E, Rossi C. Immobilization of kojic acid in ZnAl-hydroxalcalite like compounds. *J. Phys. Chem. Solids.* 2012; 73(1):94–98.
22. Gallarate M, Carlotti ME, Trotta M, Grande AE, Talarico C. Photostability of naturally occurring whitening agents in cosmetic microemulsions. *J. Cosmet. Sci.* 2004; 55:139–148. [PubMed: 15131725]
23. Lajis AF, Hamid M, Ariff AB. Depigmenting effect of Kojic acid esters in hyperpigmented B16F1 melanoma cells. *J. Biomed. Biotechnol.* 2012; 2012:952452. [PubMed: 23091364]
24. Ahn SM, Rho HS, Baek HS, Joo YH, Hong YD, Shin SS, Park YH, Park SN. Inhibitory activity of novel kojic acid derivative containing trolox moiety on melanogenesis. *Bioorg. Med. Chem. Lett.* 2011; 21(24):7466–9. [PubMed: 22071299]
25. Kaatz H, Streffer K, Wollenberger U, Peter MG. Inhibition of Mushroom Tyrosinase by Kojic Acid Octanoates. *Z. Naturforsch.* 1999; 54:70–74.
26. Manosroi A, Wongtrakul P, Manosroi J, Midorikawa U, Hanyu Y, Yuasa M, Sugawara F, Sakai H, Abe M. The entrapment of kojic oleate in bilayer vesicles. *Int. J. Pharm.* 2005; 298(1):13–25. [PubMed: 15927427]
27. Balaguer A, Salvador A, Chisvert A. A rapid and reliable size-exclusion chromatographic method for determination of kojic dipalmitate in skin-whitening cosmetic products. *Talanta.* 2008; 75(2): 407–11. [PubMed: 18371899]
28. Madhogaria S, Ahmed I. Leucoderma after use of a skin-lightening cream containing kojic dipalmitate, liquorice root extract and Mitracarpus scaber extract. *Clin. Exp. Dermatol.* 2010; 35(4):e103–5. [PubMed: 19925490]
29. Ouimet MA, Griffin J, Carbone-Howell AL, Wu WH, Stebbins ND, Di R, Uhrich KE. Biodegradable ferulic acid-containing poly(anhydride-ester): degradation products with controlled release and sustained antioxidant activity. *Biomacromolecules.* 2013; 14(3):854–61. [PubMed: 23327626]

30. Ouimet MA, Stebbins ND, Uhrich KE. Biodegradable coumaric acid-based poly(anhydride-ester) synthesis and subsequent controlled release. *Macromol. Rapid Commun.* 2013; 34(15):1231–6. [PubMed: 23836606]
31. Faig JJ, Klein S, Ouimet MA, Yu W, Uhrich KE. Attenuating Oxidative Stress Via Oxalate Ester-Containing Ferulic Acid-Based Poly(anhydride-esters) that Scavenge Hydrogen Peroxide. *Macromol. Chem. Phys.* 2016; 217(1):108–114.
32. Chen Y, Lu P, Hulme C, Shaw A. Synthesis of kojic acid-derived copper-chelating apoptosis inducing agents. *Med. Chem. Res.* 2013; 22:995–1003.
33. Schmeltzer RC, Johnson M, Griffin J, Uhrich K. Comparison of salicylate-based poly(anhydride-esters) formed via melt-condensation versus solution polymerization. *J. Biomater. Sci. Polym. Ed.* 2008; 19(10):1295–306. [PubMed: 18854123]
34. Ayouni L, Cazorla G, Chaillou D, Herbreteau B, Rudaz S, Lantéri P, Carrupt PA. Fast Determination of Lipophilicity by HPLC. *Chromatographia.* 2005; 62(5–6):251–255.
35. OECD Nuclear Energy Agency. OECD Guidelines for the Testing of Chemicals. Vol. 117. Organisation for Economic Co-Operation and Development; Paris: 2004. Organisation for Economic Cooperation and Development., Partition coefficient (1-octanol/water), High Performance Liquid Chromatography (HPLC) Method.
36. Ouimet MA, Faig JJ, Yu W, Uhrich KE. Ferulic Acid-Based Polymers with Glycol Functionality as a Versatile Platform for Topical Applications. *Biomacromolecules.* 2015; 16:2911–2919. [PubMed: 26258440]
37. Matthew E, Laskin JD, Zimmerman EA, Weinstein IB, Hsu KC, Engelhardt DL. Benzodiazepines have high-affinity binding sites and induce melanogenesis in B16/C3 melanoma cells. *Proc. Natl. Acad. Sci. U. S. A.* 1981; 78(6):3935–3939. [PubMed: 6267610]
38. Shpaisman N, Sheihet L, Bushman J, Winters J, Kohn J. One-step synthesis of biodegradable curcumin-derived hydrogels as potential soft tissue fillers after breast cancer surgery. *Biomacromolecules.* 2012; 13(8):2279–86. [PubMed: 22703560]
39. Pion F, Ducrot P-H, Allais F. Renewable Alternating Aliphatic-Aromatic Copolyesters Derived from Biobased Ferulic Acid, Diols, and Diacids: Sustainable Polymers with Tunable Thermal Properties. *Macromol. Chem. Phys.* 2014; 215(5):431–439.
40. Prudencio A, Schmeltzer RC, Uhrich KE. Effect of Linker Structure on Salicylic Acid-Derived Poly(anhydride-esters). *Macromolecules.* 2005; 38(16):6895–6900. [PubMed: 23976793]
41. Prudencio A, Faig J, Song M, Uhrich K. Phenolic Acid-based Poly(anhydride-esters) as Antioxidant Biomaterials. *Macromol. Biosci.* 2016; 16:214. [PubMed: 26425923]
42. Rho HS, Baek HS, You JW, Kim S, Lee JY, Kim DH, Chang IS. New 5-Hydroxy-2-(hydroxymethyl)-4H-pyran-4-one Derivative Has Both Tyrosinase Inhibitory and Antioxidant Properties. *Bull. Korean Chem. Soc.* 2007; 38(3):471–473.
43. Heng, KY., Kei, TY., Singh, KJ., Hairui, L., Ai-Ling, P., Lifeng, K. *Handbook of Cosmeceutical Excipients and Their Safeties.* Woodhead Publishing; New York, NY: 2014.
44. Weiser JR, Yueh A, Putnam D. Protein release from dihydroxyacetone-based poly(carbonate ester) matrices. *Acta Biomater.* 2013; 9(9):8245–53. [PubMed: 23747318]
45. Weiser JR, Zawaneh PN, Putnam D. Poly(carbonate-ester) s of dihydroxyacetone and lactic acid as potential biomaterials. *Biomacromolecules.* 2011; 12(4):977–86. [PubMed: 21401021]
46. Comisar CM, Hunter SE, Walton A, Savage PE. Effect of pH on Ether, Ester, and Carbonate Hydrolysis in High-Temperature Water. *Ind. Eng. Chem. Res.* 2008; 47:577–584.
47. Dibenedetto A, Aresta M, Giannoccaro P, Pastore C, Pápai I, Schubert G. On the Existence of the Elusive Monomethyl Ester of Carbonic Acid [CH₃OC(O)OH] at 300 K: 1H- and 13C NMR Measurements and DFT Calculations. *Eur. J. Inorg. Chem.* 2006; 2006(5):908–913.
48. Erdmann L, Uhrich KE. Synthesis and degradation characteristics of salicylic acid-derived poly(anhydride-esters). *Biomaterials.* 2000; 21:1941–1946. [PubMed: 10941915]

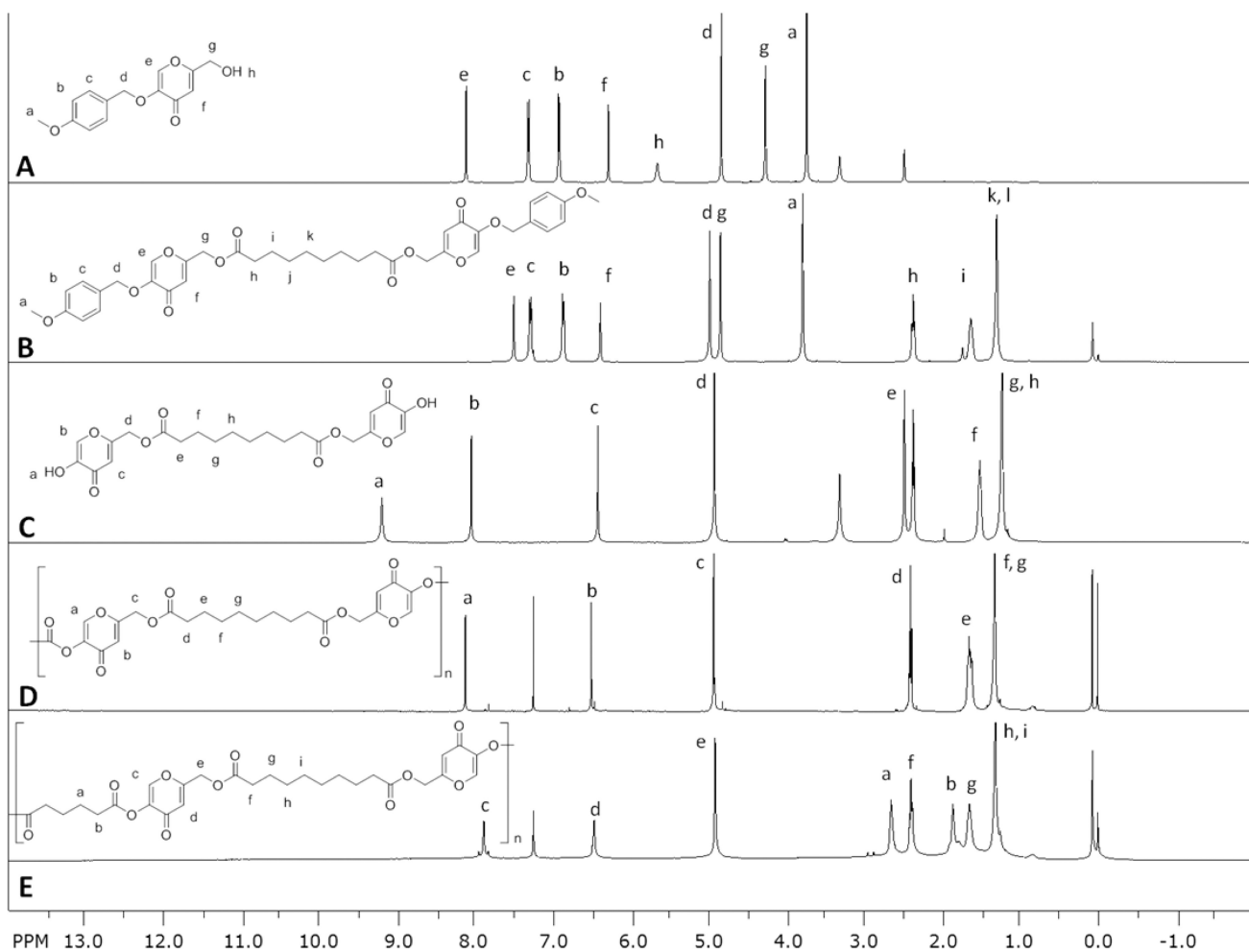


Figure 1. Representative ^1H NMR spectra comparing KA-sebacic polymers and polymer precursors. PMB-KA, **2** (A), PMB-KA (sebacate) diester, **3d** (B), KA (sebacate) dienol, **4d** (C), KA (sebacate) poly(carbonate-ester), **5d** (D), and KA (sebacate-co-adipate) polyester, **6d** (E) spectra.

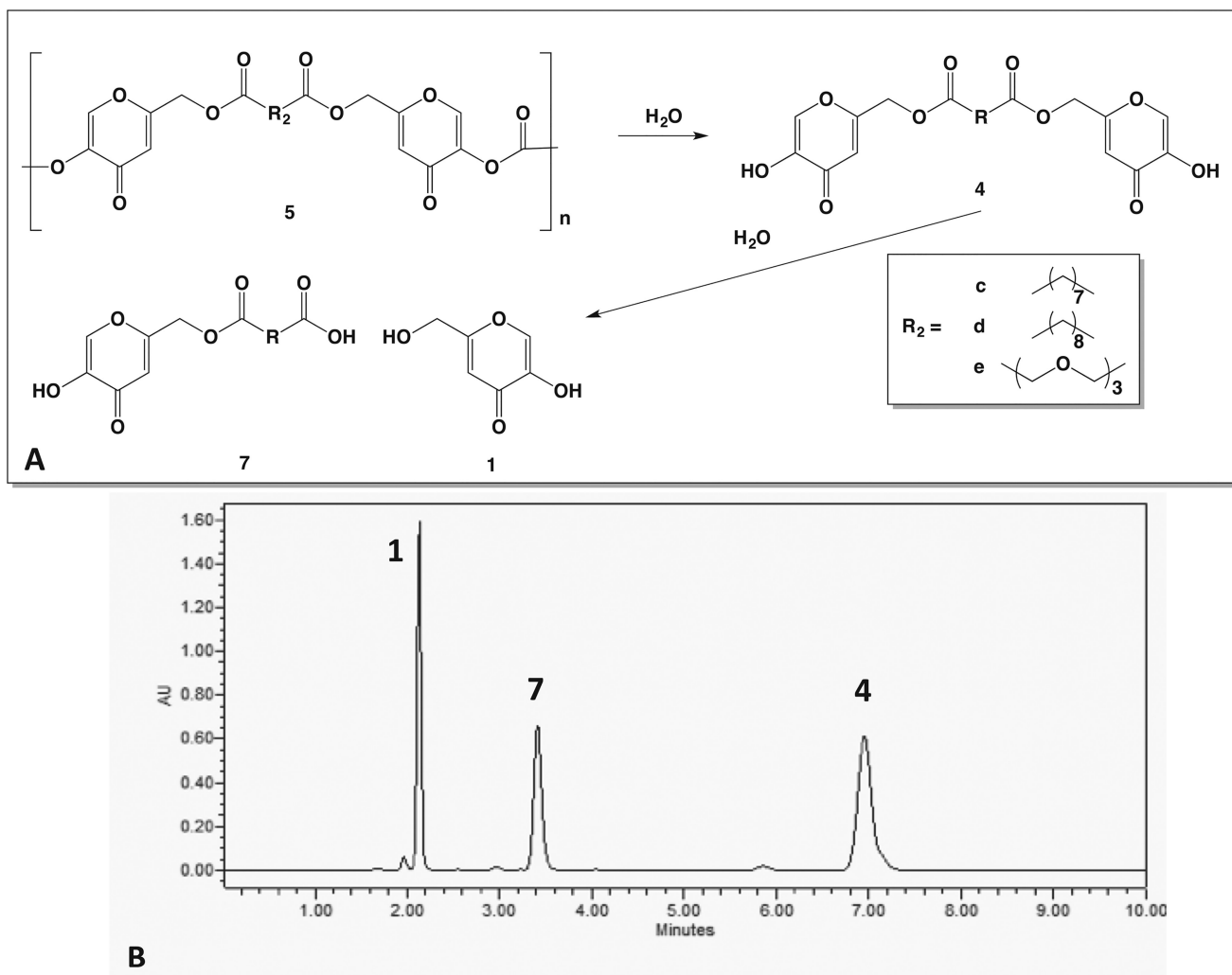


Figure 2. KA-based poly(carbonate-ester) degradation. (A). Proposed degradation pathway of poly(carbonate-ester) (B). HPLC chromatogram of 5e coating degradation after 8h under physiological conditions revealing KA (1) at 2.18, enol (7e) at 3.44, and diol (4e) at 6.95 min retention time.

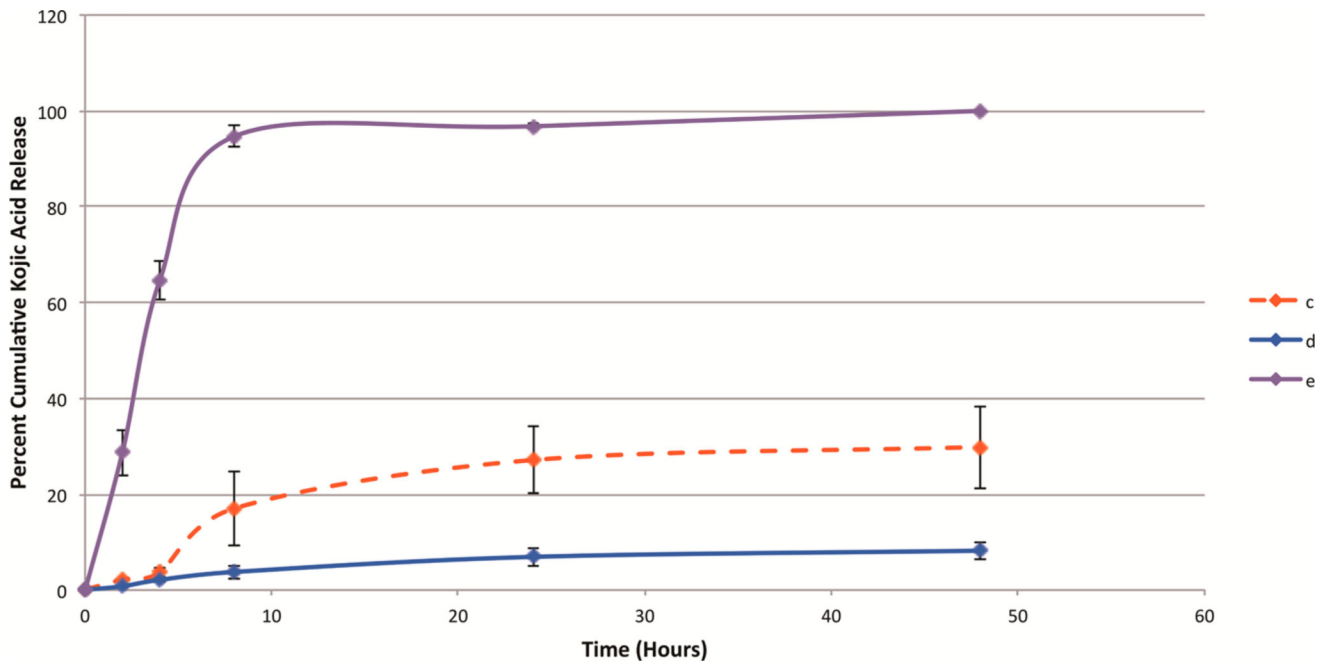


Figure 3. Release curve showing normalized release of KA over 2 days, based upon known KA concentration from KA-based poly(carbonate-ester) coatings under physiological conditions.

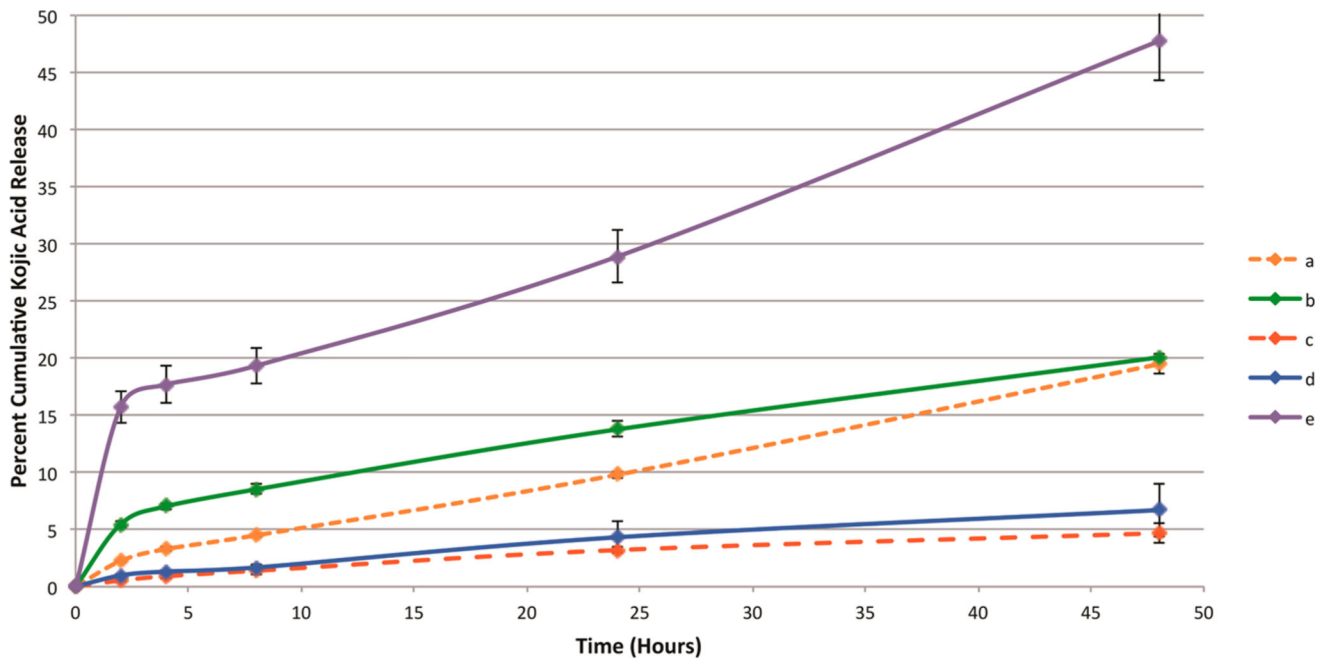


Figure 4. Release curve showing normalized release of KA over 2 days, based upon known KA concentration from KA-based polyester coatings under physiological conditions.

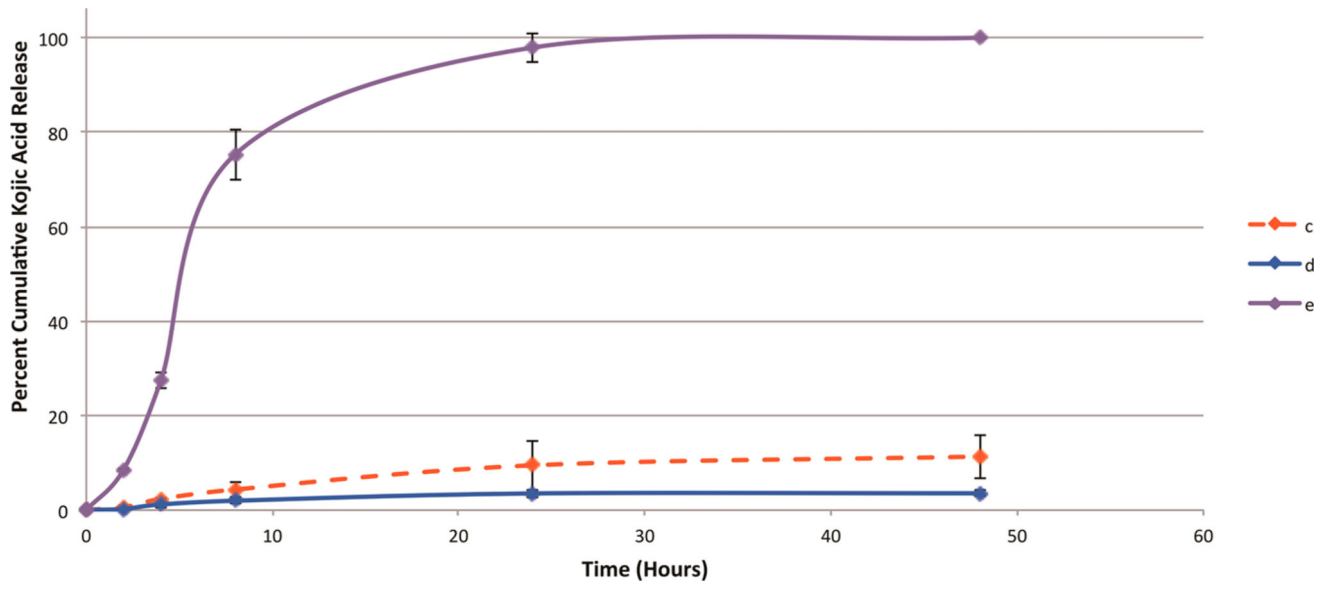


Figure 5. Release curve showing normalized release of KA over 2 days, based upon known KA concentration from KA-based poly(carbonate-ester) coatings under skin conditions.

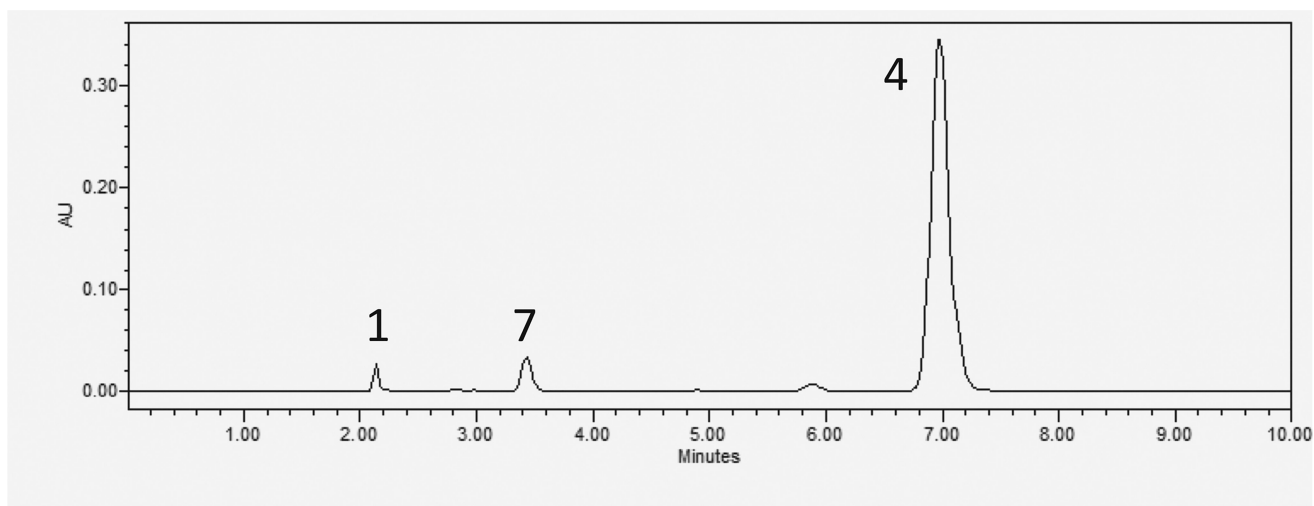


Figure 6.

Representative HPLC chromatogram of **5e** coating degradation after 8 h under skin mimic conditions releasing KA (**1**) at 2.18, enol (**7e**) at 3.44, and dienol (**4e**) at 6.95 min retention time. Predominant product is **4e**, whereas physiological conditions possessed a significantly larger amount of KA (**1**) and KA enol (**7**).

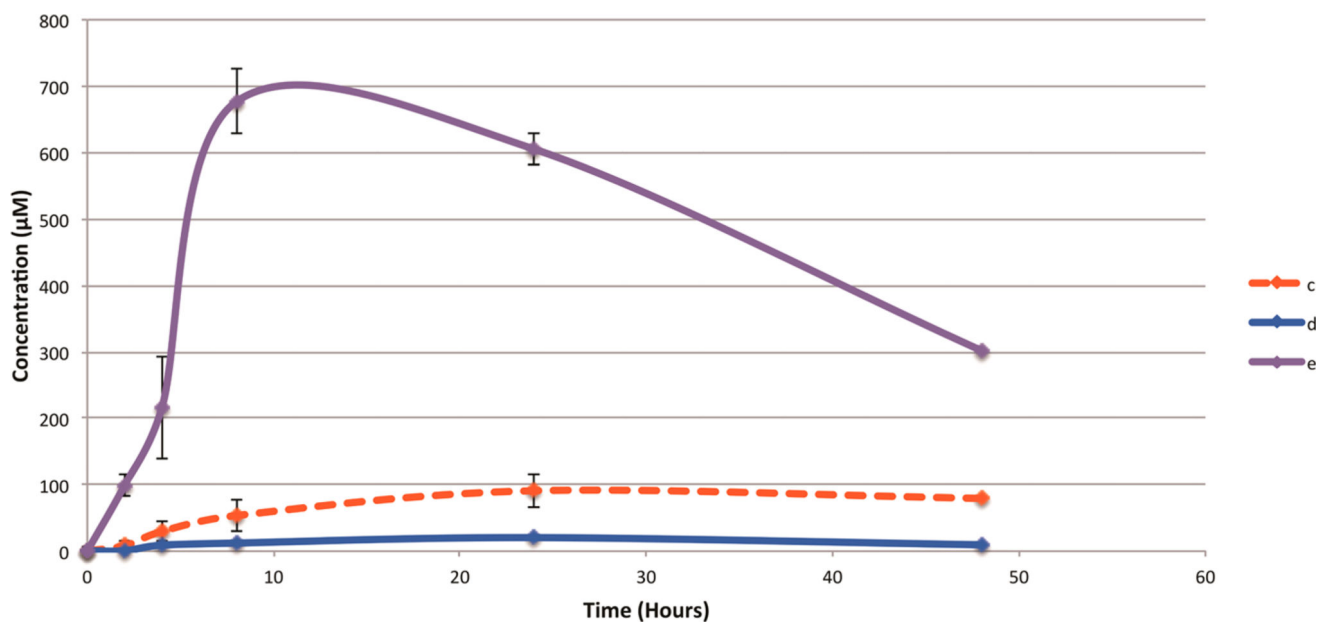


Figure 7.
Concentration of dienols (4) at each time-point of KA-based poly(carbonate-ester) degradation (5) under skin conditions.

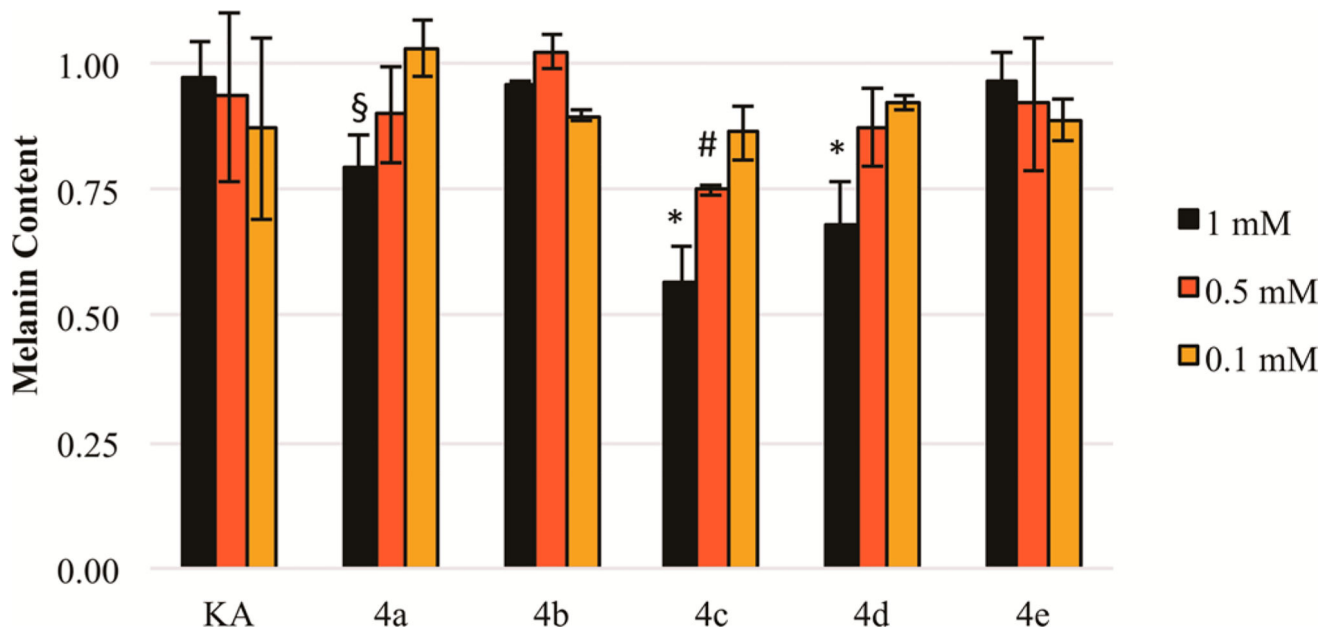
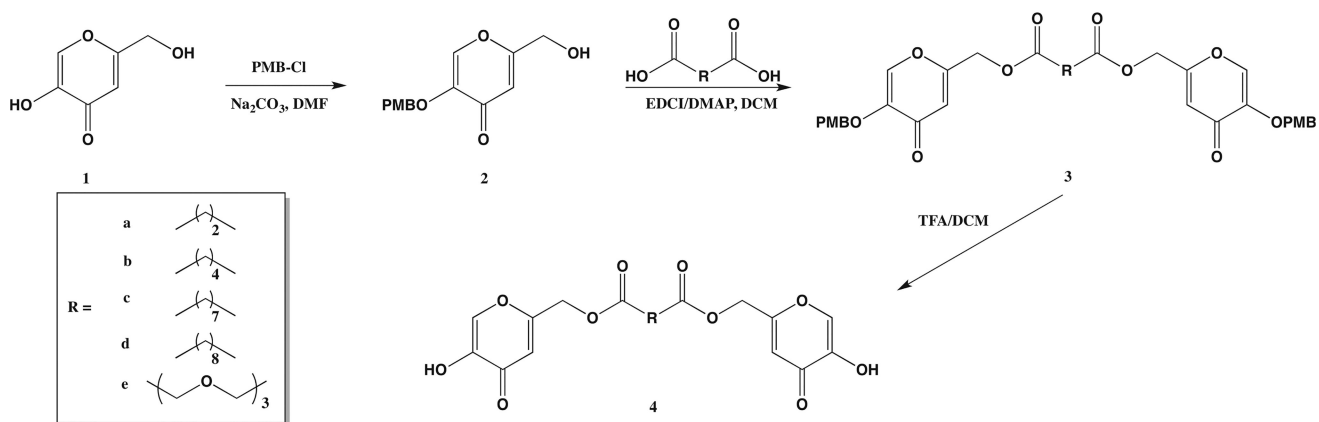
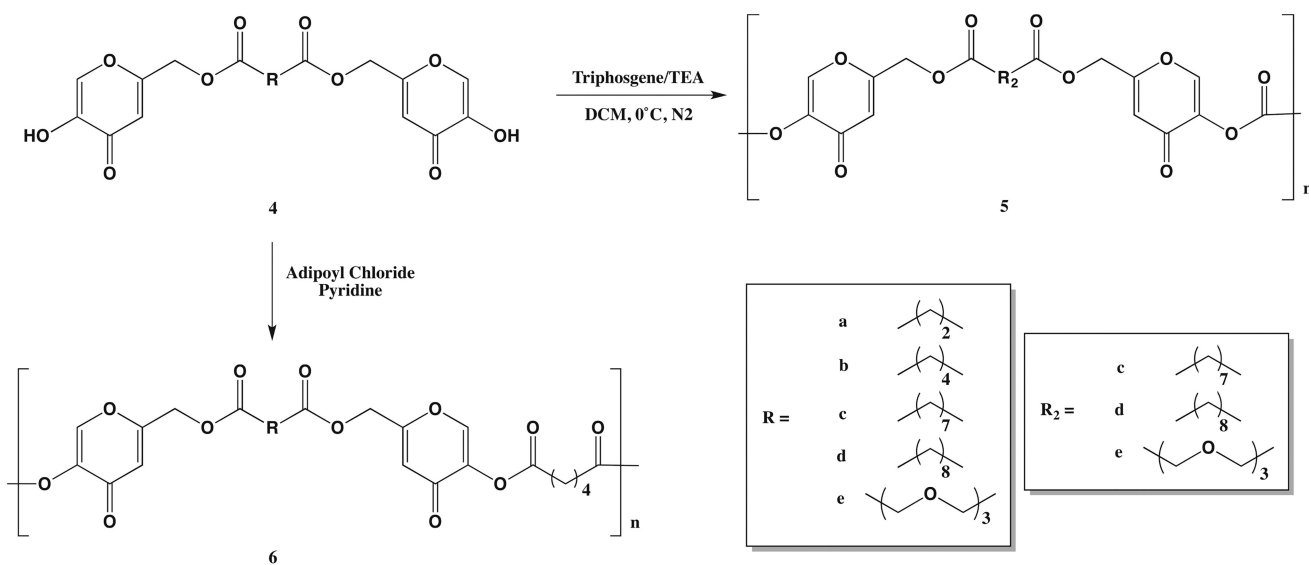


Figure 8. Melanin inhibition demonstrating enhanced activity of KA aliphatic dienol analogues, specifically **4c**, which inhibited 44% at 1 mM. * $p < 0.0001$, § $p < 0.01$, # $p < 0.05$.



Scheme 1. KA-Containing Polymer Precursor Syntheses Including PMB-KA (2), PMB-KA Diesters (3) with varying linkers (R = a–e), and KA Dienols (4) with varying linkers (R = a–e)



Scheme 2.
KA-Containing Poly(carbonate-ester) (5) and Polyester (6) Synthesis with Varying Linker Molecules (R = a-e)

Table 1Calculated log *P* Values for Dienols (4a–e) to Elucidate Lipophilicity

sample	calculated k_w	calculated log <i>P</i> values
4a	0.806	0.353
4b	2.40	1.17
4c	16.0	2.59
4d	31.6	3.10
4e	0.688	0.235

Author Manuscript

Author Manuscript

Author Manuscript

Author Manuscript

Table 2Lower IC₅₀ Values Were Observed with Aliphatic-Linked Dienols When Compared to KA

sample	IC ₅₀ (μM)	standard deviation
KA	18	± 1.2
4a	6.8	± 0.33
4b	6.0	± 0.28
4c	7.3	± 0.26
4d	14	± 1.7
4e	30	± 2.4

Author Manuscript

Author Manuscript

Author Manuscript

Author Manuscript